Unimacromolucule Exchange between Bimodal Micelles Self-Assembled by Polystyrene-*block*-Poly(acrylic acid) and Polystyrene-*block*-Poly(amino propylene-glycol methacrylate) in Water

Wangqing Zhang, Linqi Shi,* Yingli An, Lichao Gao, and Binglin He

State Key Laboratory of Adsorption and Separation Functional Polymer, Institute of Polymer Chemistry, N&T Joint Academy, Nankai University, Tianjin, 300071 China

Received: August 8, 2003; In Final Form: October 27, 2003

Unimacromolucule exchange between bimodal star micelles self-assembled by polystyrene-*block*-poly(acrylic acid) and polystyrene-*block*-poly(amino propylene-glycol methacrylate) in water has been studied by laser light scattering. Unimacromolucule exchange can take place in the mixture of the bimodal star micelle aqueous solution at 25 °C. Increasing temperature accelerates the rate of the unimacromolucule exchange. The unimacromolucule exchange between the bimodal star micelles is proved by the changes of the hydrodynamic radius (R_h), the gyration radius (R_g), and the R_g/R_h value of the mixed bimodal star micelles when the mixed bimodal micelle solution is heated at different temperatures. The reason for unimacromolucule exchange between the "frozen" bimodal star micelles is discussed, and a possible mechanism is suggested. The unimacromolucule exchange results in the formation of hybrid micelles with a more compact structure than that of typical star micelles due to the strong affinity between the functional groups in the shell-forming blocks of the copolymer chains.

1. Introduction

The micellization behavior of amphiphilic block copolymers in block-selective solvent has attracted much attention in the fundamental and applied fields of polymer science.[1−6] An important aspect of copolymer micelle research involves the dynamics of unimacromolucule exchange between micelles. For small molecular amphiphiles, unimer exchange between micelles is usual and the rate of unimer exchange is relatively fast. However, for copolymer micelles, it is usually slow for reasons such as the high molecular weight and the consequent low mobility of the chains in the cores of the micelles, as well as the low critical micelle concentration (CMC) of the block copolymers. Eisenberg et al. studied the unimacromolucule exchange between bimodal crew-cut micelles self-assembled by two block copolymers of polystyrene-*block*-poly(acrylic acid) (PS-*b*-PAA) with different block lengths in H_2O/DMF mixture by laser light scattering (LLS) and transmission electron microscopy (TEM).[7] They found that the unimacromolucule exchange was negligible when the water content was up to 11 wt %. For star micelles, the dynamic process of unimacromolucule exchange has been studied by several methods, including fluorescence and sedimentation velocity measurements.[8−11] The progress of unimacromolucule exchange is found to depend on the degree of incompatibility of the solvent and the insoluble block. For example, for micelles self-assembled by polystyrene-*b*-poly(methacrylic acid) (PS-*b*-PMAA) copolymers with different block lengths in a dioxane/water mixture, the rate of hybridization is found to be significant over the time scale of hours when the solvent is a mixture of 80 vol % dioxane and 20 vol % water. However, when the water content in the solvent mixture increases to above 30 vol %, unimacromolucule exchange between the micelles becomes negligible over a period of several days because the micelle structure is frozen.[10] In conclusion, the rate of unimacromolucule exchange between micelles, either crew-cut micelles or star micelles, decreases when the content of precipitant for the polystyrene block increases and then the rate becomes negligible when the content of precipitant further increases to some extent to freeze the micelles.

As discussed above, the micelles used to study unimacromolucule exchange were prepared from the same type of block copolymers differing only in the relative block length; thus, the interaction between the shell-forming chains of the micelles was very weak because the shell of the micelles was composed of the same block chains and there was no strong affinity between the polymer chains. Can unimacromolucule exchange also take place between the considered "frozen" star micelles if there exists strong affinity between the shell-forming chains of polymers? In this article, we study the unimacromolucule exchange between the bimodal micelles self-assembled by polystyrene-*block*-poly(acrylic acid) (PS_{24}-*b*-PAA_{116}) and polystyrene-*block*-poly(amino propylene-glycol methacrylate) (PS_{51}-*b*-$PAPMA_{140}$) in water by LLS. We find that unimacromolucule exchange can take place in the mixture of the bimodal star micelle aqueous solution. Furthermore, the special structure of the hybrid micelles resulted from the unimacromolucule exchange is also discussed.

2. Experimental Section

2.1. Polymer Samples. Polystyrene-*block*-poly(methyl acrylate) (PS_{24}-*b*-PMA_{116}) was synthesized by atom transfer radical polymerization (ATRP).[12] The polydispersity index (PDI) of PS_{24}-*b*-PMA_{116} measured by gel permeation chromatography (GPC) was 1.28. The composition of block copolymer PS_{24}-*b*-PMA_{116} was determined from the ratio of the ^1H NMR intensities of the OCH_3 signal at $\delta = 3.7$ and the aromatic signal

* To whom correspondence should be addressed. Phone: 0086-22-23506103. E-mail: shilinqi@nankai.edu.cn.

10.1021/jp036355x CCC: $27.50
Published on Web 12/09/2003

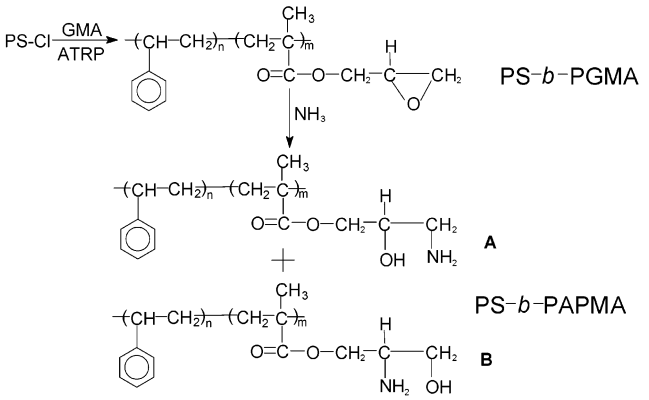

Figure 1. Polymer structure and the preparation for PS_{51}-*b*-$PAPMA_{140}$.

at $\delta = 6.6-7.3$ of the block copolymer. 2 g of PS_{24}-*b*-PMA_{116} was hydrolyzed in 50 mL of 20 wt % NaOH aqueous solution at 90 °C for 72 h. The product, PS_{24}-*b*-PAA_{116}, was deposited by slowly adding the polymer solution into 40 mL of 33 vol % hydrochloric acid. The precipitate was centrifugated and washed with 5 vol % dilute hydrochloric acid and deionized water each for six times, respectively. The product was then dried at 50 °C in a vacuum oven for 24 h.

PS_{51}-*b*-$PAPMA_{140}$ was prepared by hydrolysis of polystyrene-*b*-poly(glycidyl methacrylate) (PS_{51}-*b*-$PGMA_{140}$), which was synthesized by ATRP and the PDI of the block copolymer measured by GPC was 1.42, in an excessive amount of 17 wt % ammonia aqueous solution/butanone mixture at 60 °C. The preparation steps and the polymer structure of PS_{51}-*b*-$PAPMA_{140}$ are shown in Figure 1. A more detailed description can be found in the Supporting Information.

2.2. Preparation of the Micelle Solutions. PS_{24}-*b*-PAA_{116} or PS_{51}-*b*-$PAPMA_{140}$ was dissolved in *N*,*N*-dimethylformamide (DMF) to make a copolymer solution at 0.20 mg/mL. The PS_{24}-*b*-PAA_{116} or PS_{51}-*b*-$PAPMA_{140}$ micelle solution was prepared by first adding 2.0 mL of the copolymer solution into 20 mL of water at rate of one drop (about 0.007 mL) every 10 s by a microsyringe with stirring. After 24 h, the solution was dialyzed against water for 4 days to remove DMF to produce a micelle solution with polymer concentration at 20 μg/mL. The mixed bimodal micelles were prepared by first dropping 2.0 mL of 0.20 mg/mL PS_{24}-*b*-PAA_{116} DMF solution into 20 mL of water, and then 2.0 mL of 0.20 mg/mL PS_{51}-*b*-$PAPMA_{140}$ DMF solution was added after 24 h. At last, the mixed bimodal micelles solution was dialyzed against water for 4 days to remove DMF to produce a micelle solution with PS_{24}-*b*-PAA_{116} and PS_{51}-*b*-$PAPMA_{140}$ concentration at 20 μg/mL. For the LLS measurement, about 1 mL of the micelle solution was first filtered with a 0.2 μ Millipore filter into a clean scintillation vial and then step by step heated at a given temperature for a given time and then measured at last.

2.3. LLS Measurement. Dynamic laser light scattering (DLLS) and static laser light scattering (SLLS) experiments were performed on a laser light scattering spectrometer (BI-200SM) equipped with a digital correlator (BI-9000AT) at 532 nm. In DLLS measurements, the Laplace inversion of a measured intensity−intensity time correlation function $G^{(2)}(t, q)$ in the self-beating mode can result in a line-width distribution $G(\Gamma)$. For a pure diffusive relation, $G(\Gamma)$ can be transferred into a transitional diffusion coefficient distribution $G(D)$ because $\Gamma/q^2_{\theta\to 0, C\to 0} \to D$, or a hydrodynamic radius distribution $f(R_h)$ via the Stokes−Einstein equation

$$R_h = k_B T/(6\pi\eta D) \qquad (1)$$

where k_B, T, and η are the Boltzmann constant, the absolute temperature, and the solvent viscosity, respectively. The detail methods can be seen as described elsewhere.[13−15] In the present study, $\Gamma/q^2_{\theta\to 0}$ or D^0 of the micelles at given concentration is calculated by extrapolating q^2 to 0, and then the hydrodynamic radius R_h^0 or the hydrodynamic radius distribution $f(R_h)$ of the micelles at given polymer concentration is further calculated from eq 1.

The radius of gyration (R_g) is calculated from SLLS. On the basis of SLLS theory, for a relatively high dilute macromolecule solution or strongly interacting particles (for example, polyelectrolytes) at polymer concentration C (g/mL) and at the scattering angle θ, the angular dependence of the excess absolute average scattered intensity, known as the excess Rayleigh ratio $[R(\theta,C)]$, can be approximated as

$$[KC/R(\theta,C)]^{0.5} = [1/M_W]^{0.5}[1 + (R_g^2 q^2)/6][1 + A_2 C] \quad (2)$$

where K is the optical constant and $K = 4\pi^2 n^2 (dn/dc)^2/(N_A \lambda_0^4)$ with N_A, n, and λ_0 being Avogadro's number, the solvent refractive index, and the wavelength of the laser, respectively, dn/dc is the specific refractive index increment, A_2 is the second virial coefficient, M_W is weight-average molecular weight, R_g is the square z-average radius of gyration, q is the magnitude of the scattering wave vector, and $q = (4\pi n/\lambda_0)\sin(\theta/2)$. For a given very dilute polymer solution, eq 2 can be expressed as

$$[KC/R(\theta,C)]^{0.5} \approx [1/M_W]^{0.5}[1 + (R_g^2 q^2)/6] \qquad (3)$$

In the present study, because of the very dilute polymer concentration, the apparent radius of gyration was calculated after measuring $R(\theta,C)$ at a set of θ on eq 3.

3. Results and Discussion

Figure 2A shows the plots of the translational diffusion coefficient D and the hydrodynamic diameter D_h of PS_{24}-*b*-PAA_{116} micelles (a), PS_{51}-*b*-$PAPMA_{140}$ micelles (b), and the mixed bimodal micelles (c) versus q^2 at 25 °C, respectively. In the DLLS study, the translational diffusion coefficients D of the three kinds of micelles at different scattering angles are measured, which is shown in Figure 2B. The translational diffusion coefficient D of PS_{24}-*b*-PAA_{116} micelles shown in Figure 2A ranges from 1.202×10^{-7} to 1.227×10^{-7} cm^2/s, and the calculated hydrodynamic diameter shown in Figure 2B ranges from 40.8 to 40.0 nm with the scattering angle ranging from 50° to 130°, respectively. By extrapolating q^2 to 0, the translational diffusion coefficient and the hydrodynamic diameter of the PS_{24}-*b*-PAA_{116} micelles at a given polymer concentration, which are called D^0 and D_h^0, are calculated, and the values are 1.210×10^{-7} cm^2/s and 40.5 nm, respectively. Clearly, the value of D_h^0 is very close to D_h, and thus, the scattering angle dependence of the PS_{24}-*b*-PAA_{116} micelles can be neglected. We think the reason is that the micelles are spherical and the size of the micelles is small enough. Similar to the PS_{24}-*b*-PAA_{116} micelles, the D and D_h of the PS_{51}-*b*-$PAPMA_{140}$ micelles and the mixed bimodal micelles change very little with scattering angle or q^2 as shown in Figure 2, part A and B. The D_h^0 of the PS_{51}-*b*-$PAPMA_{140}$ micelles and the mixed bimodal micelles is 48.9 and 55.6 nm, respectively. Thus, in the following further study, the value of D_h of the PS_{24}-*b*-PAA_{116} micelles, PS_{51}-*b*-$PAPMA_{140}$ micelles, and the mixed bimodal micelles measured at 90° scattering angle was used unless specified otherwise.

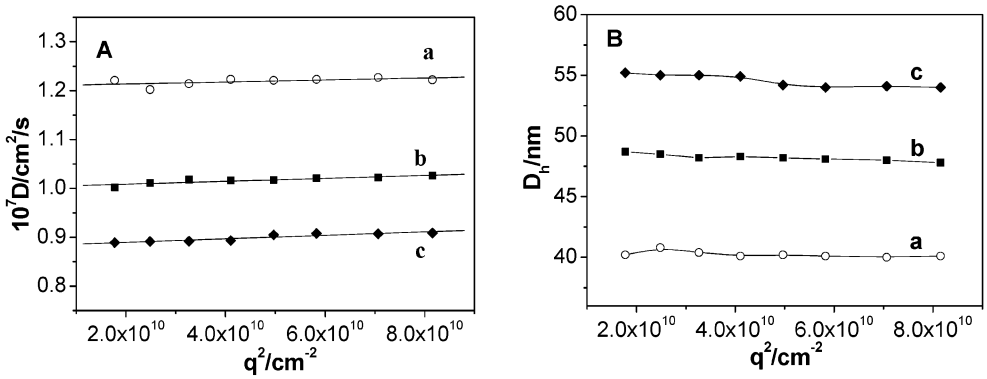

Figure 2. Plots of the translational diffusion coefficient D (A) and hydrodynamic diameter D_h (B) versus q^2 at 25 °C of PS_{24}-*b*-PAA_{116} micelles (a) and PS_{51}-*b*-$PAPMA_{140}$ micelles (b) and the mixed bimodal micelles after the mixed micelle solution kept for 1 day (c).

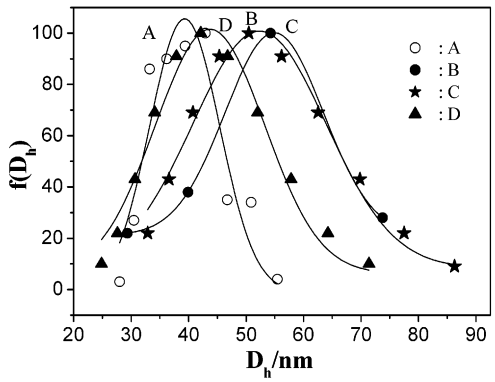

Figure 3. Diameter distributions of the micelles self-assembled by PS_{24}-*b*-PAA_{116} (A), PS_{51}-*b*-$PAPMA_{140}$ (B), and the bimodal micelles after kept for 1 day (C) and 60 days (D) in water, where all of the diameter distributions are measured at 90° scattering angle at 25 °C.

The hydrodynamic diameter distributions of the micelles self-assembled by PS_{24}-*b*-PAA_{116} and PS_{51}-*b*-$PAPMA_{140}$ and the mixed bimodal micelles after kept for 1 day or 60 days in water are shown in Figure 3A−D. Clearly, each of the micelles self-assembled by PS_{24}-*b*-PAA_{116} and PS_{51}-*b*-$PAPMA_{140}$ shows a narrow diameter distribution with diameter ranging from 28.0 to 55.5 nm and 29.4 to 73.8 nm and the average diameters are 40.2 and 48.3 nm, respectively. The mixed bimodal micelle after the micelle solution kept 1 day has a relatively broad diameter distribution as shown in Figure 3C, where the diameter ranges from 32.9 to 86.3 nm and the average diameter is about 54.2 nm. Clearly, the diameter distribution of the bimodal micelles is not similar to either of the two individual copolymer micelles or the sum of the two diameter distributions in Figure 3, parts A and B, but is a little broadened. Moreover, the average diameter of the bimodal micelles is a little larger than either of the two individual micelles. This means association between PS_{24}-*b*-PAA_{116} micelles and PS_{51}-*b*-$PAPMA_{140}$ micelles takes place, which results in the formation of larger supermicelles in the system when mixing the two individual polymer micelle solutions at 25 °C. To further study the mixed bimodal micelles, the mixed bimodal micelle solution was kept for 60 days at room temperature until the hydrodynamic diameter measured by DLLS almost remains constant. The diameter distribution is shown in Figure 3D. The mixed bimodal micelle has a narrower diameter distribution than that kept for 1 day as shown in Figure 3C, where the diameter ranges from 24.8 to 71.4 nm and the average diameter is about 45.3 nm. Clearly, the diameter of the mixed bimodal micelles decreases when the micelle solution was kept for 60 days at room temperature and the average diameter locates between those of the PS_{24}-*b*-PAA_{116} micelles and PS_{51}-*b*-$PAPMA_{140}$ micelles. This suggests that unimacromolucule exchanges have taken place between the bimodal micelles and the hybrid micelles are formed. However, it should be pointed out that the rate of the unimacromolucule exchange between the mixed bimodal micelles of PS_{24}-*b*-PAA_{116} micelles and PS_{51}-*b*-$PAPMA_{140}$ micelles is slow at room temperature and the diameter of the mixed bimodal micelles does not change much over the time scale of hours until the mixed bimodal solution have been kept for about 60 days.

Generally, unimacromolucule exchange between "frozen" micelles, for example PS_{170}-*b*-PAA_{33} micelles and PS_{1140}-*b*-PAA_{165} in water, does not happen easily.[7] That unimacromolucule exchange can take place between the considered "frozen" PS_{24}-*b*-PAA_{116} and PS_{51}-*b*-$PAPMA_{140}$ micelles at room temperature is possibly due to three reasons that are discussed below. First, there exists a strong affinity between the shell-forming chains of PS_{24}-*b*-PAA_{116} and PS_{51}-*b*-$PAPMA_{140}$ because of the amino and hydroxyl groups in PS_{51}-*b*-$PAPMA_{140}$ chains and carboxyl groups in PS_{24}-*b*-PAA_{116} chains. The affinity is partly due to the Coulombic attraction between the protonated amino groups ($-NH_3^+$) and ionized carboxyl groups ($-COO-$) and partly due to the hydrogen bond between amino or hydroxyl groups and carboxyl groups. The strong affinity may promote unimacromolucule exchange and association between PS_{24}-*b*-PAA_{116} micelles and PS_{51}-*b*-$PAPMA_{140}$ micelles in water as discussed above. The second reason is due to the composition of the two block copolymers. Both PS_{24}-*b*-PAA_{116} and PS_{51}-*b*-$PAPMA_{140}$ have longer shell-forming blocks compared to the core-forming block of polystyrene, which results in a relatively high CMC of the polymers in water and thus makes a relatively fast equilibrium between the unimer chains and the micelles. Third, the structure of the PS_{24}-*b*-PAA_{116} micelles and PS_{51}-*b*-$PAPMA_{140}$ micelle solutions is not as compact as typical crew-cut micelles. Figure 4 shows the Berry plots of $[I^{-1}]^{0.5}$ of the PS_{24}-*b*-PAA_{116} micelles and PS_{51}-*b*-$PAPMA_{140}$ micelles versus q^2 at 25 °C, where I is the scattering intensity of the sample at a scattering angle θ. Form the fit lines in Figure 4, the values of R_g of the PS_{24}-*b*-PAA_{116} micelles and PS_{51}-*b*-$PAPMA_{140}$ micelles in water at 25 °C are calculated as $R_g = (6S/T)^{0.5}$, where S is the slope and T is the intercept of the fit line. The values of R_g of PS_{24}-*b*-PAA_{116} micelles and PS_{51}-*b*-$PAPMA_{140}$ micelles are 21.1 and 23.0 nm, respectively. Thus, the R_g/R_h values of PS_{24}-*b*-PAA_{116} micelles and PS_{51}-*b*-$PAPMA_{140}$ micelles in water at 25 °C are 1.050 and 0.952, respectively, which are much larger than that of crew-cut micelles. This suggests the structure of the PS_{24}-*b*-PAA_{116} micelles and PS_{51}-*b*-$PAPMA_{140}$ micelles in water at 25 °C are relatively incompact. This incompact structure of the PS_{24}-*b*-PAA_{116} micelles and PS_{51}-*b*-$PAPMA_{140}$

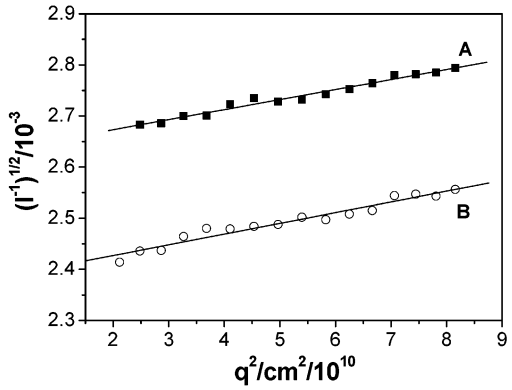

Figure 4. Berry plots of $[I^{-1}]^{0.5}$ of the PS_{24}-*b*-PAA_{116} micelles (A) and PS_{51}-*b*-$PAPMA_{140}$ micelles (B) in water at 25 °C, respectively.

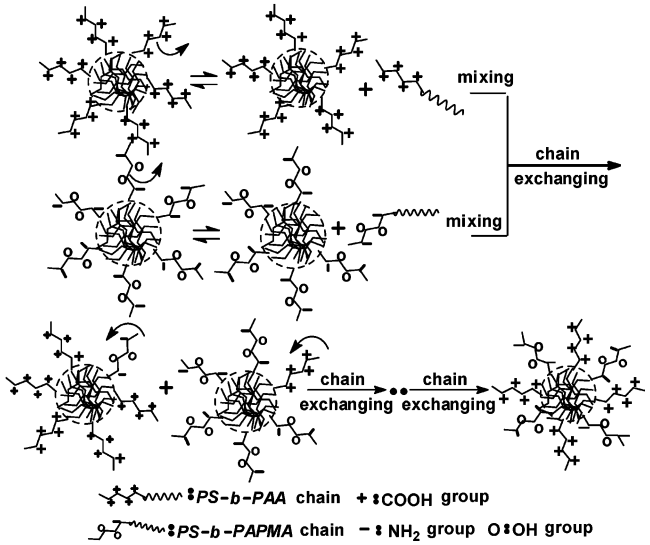

Figure 5. Possible mechanism for formation of the hybrid micelles from unimacromolucule exchange between PS_{51}-*b*-$PAPMA_{140}$ micelles and PS_{24}-*b*-PAA_{116} micelles in water.

micelles facilitates the unimacromolucule exchange between the mixed bimodal micelles in water at room temperature.

In conclusion, three essential factors promote the unimacromolucule exchange between the mixed bimodal micelles and the formation of the hybrid micelles in water at room temperature. The process and mechanism of the unimacromolucule exchange between the bimodal micelles are shown in Figure 5.

It is well-known that temperature is an important factor for many physical and chemical processes such as chain exchange. Clearly, temperature increasing will accelerate the rate of unimacromolucule exchange between the bimodal micelles. For block copolymer PS_{24}-*b*-PAA_{116} and PS_{51}-*b*-$PAPMA_{140}$, the polymerization degree of the core-forming block, the PS block, is very small, and the glass temperatures of the PS cores of the bimodal micelles are approximately 50 and 70 °C, respectively.[16] At a temperature above 50 °C, the glassy nature of the PS cores of the bimodal micelles is greatly bettered and the motility of the polymer chains is activated, which will accelerate the unimacromolucule exchange between PS_{24}-*b*-PAA_{116} and PS_{51}-*b*-$PAPMA_{140}$ micelles. The curves in Figure 6 show the average hydrodynamic diameter of PS_{24}-*b*-PAA_{116} micelles (Figure 6A), PS_{51}-*b*-$PAPMA_{140}$ micelles (Figure 6B), and the mixture of the bimodal micelles (Figure 6C) when heated at different temperatures for 60 min. The results show that the average hydrodynamic diameters of PS_{24}-*b*-PAA_{116} micelles and PS_{51}-*b*-$PAPMA_{140}$ micelles increase slightly when the temperature

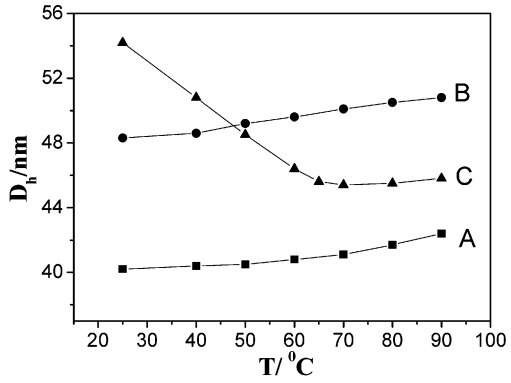

Figure 6. Average hydrodynamic diameter of PS_{24}-*b*-PAA_{116} micelles (A), PS_{51}-*b*-$PAPMA_{140}$ micelles (B), and the mixture of the above two micelles solutions (C) when heating for 60 min at different temperature.

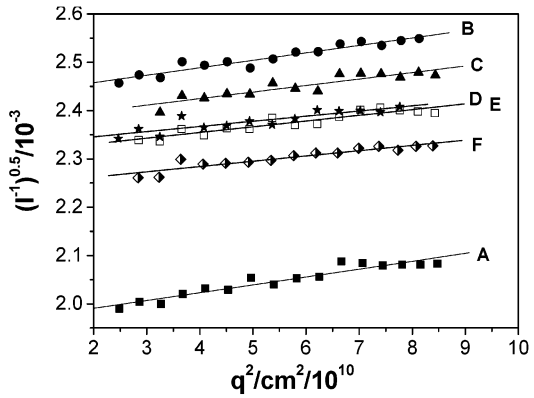

Figure 7. Berry plots of $[I^{-1}]^{0.5}$ of mixed bimodal micelles versus q^2 when the mixed bimodal micelle solution was step by step heated at 25 °C (A), 40 °C (B), 50 °C (C), 60 °C (D), 65 °C (E), and 90 °C (F) for 60 min, respectively.

increasing from 25 to 90 °C, which is possibly due to polymer chains stretching. Whereas, the average hydrodynamic diameter of the mixture of the bimodal micelles decreases from 54.2 to 45.4 nm when the temperature increase from 25 to 70 °C and then increases slightly from 45.4 to 45.8 nm with the temperature increasing from 70 to 90 °C at last. Clearly, the average hydrodynamic diameter change indicates the unimacromolucule exchange between the bimodal micelles. The results suggest that temperature increasing can greatly accelerate the rate of unimacromolucule exchange between PS_{24}-*b*-PAA_{116} and PS_{51}-*b*-$PAPMA_{140}$ micelles. At temperatures from 65 to 80 °C, the average hydrodynamic diameter of the micelles is almost a constant, which is about 45.4 nm, that is to say, the unimacromolucule exchange is almost fulfilled and most of the bimodal micelles translate into monomodal hybrid micelles. When the temperature is further increased to 90 °C, the average hydrodynamic diameter increases slightly, which is possibly due the polymer chains stretching similar to the individual micelles self-assembled by PS_{24}-*b*-PAA_{116} and PS_{51}-*b*-$PAPMA_{140}$ as discussed above.

Besides, the radius of gyration (R_g) of the mixed bimodal micelles was also measured basing on eq 3 to study the unimacromolucule exchange between PS_{51}-*b*-$PAPMA_{140}$ micelles and PS_{24}-*b*-PAA_{116} micelles in water. Figure 7 shows the Berry plots of $[I^{-1}]^{0.5}$ of mixed bimodal micelles versus q^2 when the mixed bimodal micelle solution was heated at different temperature, where I is the scattering intensity of the samples at a scattering angle θ.

Form the fit lines in Figure 7, the values of R_g of the mixed bimodal micelles when heated at 25, 40, 50, 60, 65, and 90 °C

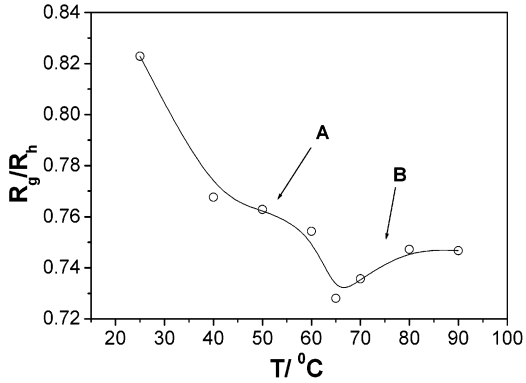

Figure 8. R_g/R_h value of the bimodal micelles when step by step heated at different temperature for 60 min.

for 60 min are calculated as $R_g = (6S/T)^{0.5}$, and the values of R_g are 22.3, 19.5, 18.5, 17.5, 16.6, and 17.1 nm, respectively. The values of R_g of the mixed bimodal micelles are also measured and calculated when the micelle solution was heated at 70 ($R_g = 16.7$ nm) and 80 °C ($R_g = 17.0$ nm) for 60 min, but the fit lines are not shown in Figure 7 because they almost overlap with line E or line F. The results show that the gyration radius of the mixed bimodal micelles decreases from 22.3 to 16.6 nm when the temperature is increased from 25 to 65 °C, and then it increases from 16.6 to 17.1 nm with the temperature ranging from 65 to 90 °C, which is very similar to the change of the hydrodynamic diameter of the mixed bimodal micelles as discussed above.

It is well-known that the value of R_g/R_h can reveal the morphology of polymer chains in dilute solution.[15,17] The curve in Figure 8 shows the R_g/R_h value of the bimodal micelles when heated at different temperatures for 60 min. According to the slope of the curve in different regions, the curve is divided into 2 segments of A (from 25 to 65 °C) and B (from 65 to 90 °C) as indicated in Figure 8. At the A segment, the R_g/R_h value of the mixture of the bimodal micelles quickly decreases from 0.822 to 0.728, which indicates the structure of the mixture of PS_{51}-*b*-$PAPMA_{140}$ micelles and PS_{24}-*b*-PAA_{116} micelles has changed much due to the unimacromolucule exchange between the bimodal micelles. At about 65 °C, the unimacromolucule exchange between PS_{51}-*b*-$PAPMA_{140}$ micelles and PS_{24}-*b*-PAA_{116} micelles is complete and the hybrid micelles are formed. This also suggests that the rate of unimacromolucule exchange between PS_{51}-*b*-$PAPMA_{140}$ micelles and PS_{24}-*b*-PAA_{116} micelles is relatively fast at 65 °C, because the solution was only heated for several hours at a temperature below 65 °C. At the B segment, the R_g/R_h value of the hybrid micelles increases slightly, which is possibly due to the polymer chains stretching at high temperature. Clearly, the results are well consistent with those discussed above.

Because of the strong affinity among the shell-forming block chains, great difference between the hybrid micelles and the two star micelles of PS_{51}-*b*-$PAPMA_{140}$ and PS_{24}-*b*-PAA_{116} is expected. The remarkable nature of the hybrid micelles is that the R_g/R_h value of the hybrid micelles is about 0.728, which is even much less than predicted for a rigid uniform sphere (~0.775),[17] while the R_g/R_h values of PS_{24}-*b*-PAA_{116} micelles and PS_{51}-*b*-$PAPMA_{140}$ are 1.050 and 0.952, respectively. This possibly indicates the compact structure of the hybrid micelles due to the strong affinity between the shell-forming chains of PS_{24}-*b*-PAA_{116} and PS_{51}-*b*-$PAPMA_{140}$.

4. Conclusions

The unimacromolucule exchange between the micelles self-assembled by PS_{24}-*b*-PAA_{116} and PS_{51}-*b*-$PAPMA_{140}$ in water was studied by LLS. When mixing of the bimodal micelle solutions at 25 °C, unimacromolucule exchange between the PS_{24}-*b*-PAA_{116} micelles and the PS_{51}-*b*-$PAPMA_{140}$ micelles takes place and the average hydrodynamic radius of the mixed micelles changes, although the individual bimodal micelles are considered to be frozen in general opinion.[7−11] The unimacromolucule exchange between the bimodal micelles results in the formation of the hybrid micelles with special structure. That the unimacromolucule exchange can take place is ascribed to the strong affinity between the shell-forming chains of PS_{24}-*b*-PAA_{116} and PS_{51}-*b*-$PAPMA_{140}$, the longer shell-forming block length compared to the core-forming block, and the incompact structure of PS_{24}-*b*-PAA_{116} micelles and PS_{51}-*b*-$PAPMA_{140}$ micelles, respectively. Temperature increasing can greatly accelerate the rate of unimacromolucule exchange between PS_{24}-*b*-PAA_{116} and PS_{51}-*b*-$PAPMA_{140}$ micelles. At a temperature of about 65 °C, the unimacromolucule exchange rate is relative fast and hybrid micelles are formed. During the unimacromolucule exchange, the average hydrodynamic radius (R_h) of the mixture of the PS_{24}-*b*-PAA_{116} and PS_{51}-*b*-$PAPMA_{140}$ micelles first decreases quickly when the temperature increases from 25 to 65 °C and then increases slightly when the temperature increases from 65 to 90 °C. The gyration radius (R_g) and the R_g/R_h value of the mixed bimodal micelles also change with temperature, which further confirms the unimacromolucule exchange.

Acknowledgment. The financial support by the National Natural Science Foundation of China (No. 50273015) and Chinese Education Ministry Foundation for Nankai University and Tianjin University Joint Academy is gratefully acknowledged.

Supporting Information Available: Text giving synthetic procedures and characterization of PS_{51}-*b*-$PAPMA_{140}$ and PS_{51}-*b*-$PGMA_{140}$, and figures showing ^{1}HNMR and FTIR of PS_{51}-*b*-$PAPMA_{140}$ and PS_{51}-*b*-$PGMA_{140}$. This material is available free of charge via the Internet at http://pubs.acs.org.

References and Notes

(1) Liu, G.; Ding, J.; Guo, A.; Herfort, M.; Bazett-Jones, D. *Macromolecules* **1997**, *30*, 1851.
(2) Yan, X.; Liu, F.; Li, Z.; Liu, G. *Macromolecules* **2001**, *34*, 9112.
(3) Zhang L.; Eisenberg, A. *Science* **1995**, *268*, 1728.
(4) Zhang L.; Eisenberg, A. *Macromolecules* **1996**, *29*, 8805.
(5) Zhang L.; Eisenberg, A. *Macromolecules* **1999**, *32*, 2239.
(6) Jenekhe, S. A.; Chen, X. L. *Science* **1999**, *283*, 372.
(7) Zhang, L.; Shen, H.; Eisenberg, A. *Macromolecules* **1997**, *30*, 1001.
(8) Prochazka, K.; Bednar, B.; Mukhtar, E.; Svoboda, P.; Trnena, J.; Almgren, M. *J. Phys. Chem.* **1991**, *95*, 4563.
(9) Wang, Y.; Kausch, C. M.; Chun, M.; Quirk, R. P.; Mattice, W. L. *Macromolecules* **1995**, *28*, 904.
(10) Tian, M.; Qin, A.; Ramireddy, C.; Webber, S. E.; Munk, P.; Tuzar, Z.; Prochazka, K. *Langmuir* **1993**, *9*, 1741.
(11) Pacovska, M.; Prochazka, K.; Tuzar, Z.; Munk, P. *Polymer* **1993**, *34*, 4585.
(12) Gao, L.; Shi, L.; Zhang W.; Gao, J.; He, B. *Chem. J. Chin. Univ.* **2001**, *10*, 224.
(13) Tu, Y.; Wan, X.; Zhang D.; Zhou, Q.; Wu, C. *J. Am. Chem. Soc.* **2000**, *122*, 10201.
(14) Zhang, Y.; Li, M.; Fang, Q.; Zhang, Y.-X.; Jiang, M.; Wu, C. *Macromolecules* **1999**, *31*, 2527.
(15) Wu, C.; Siddiq, M.; Woo, K. *Macromolecules* **1995**, *28*, 4914.
(16) O'Driscoll, K.; Sanayei, R. A. *Macromolecules* **1991**, *24*, 4479.
(17) Wu, C.; Zhou, S. *Phys. Rev. Lett.* **1996**, *77*, 3053.